2007 IEEE International Conference on
Robotics and Automation
Roma, Italy, 10-14 April 2007

Singularity Avoidance for the 3-RRR Mechanism Using Kinematic Redundancy

Sung-Hoon Cha, Ty A. Lasky, Senior Member, IEEE, and Steven A. Velinsky

Abstract*—Based on its simple structure, base-fixed actuators, high payload capacity, high accuracy, and high mechanical rigidity, the 3-RRR mechanism is a valuable planar parallel manipulator. However, the 3-RRR mechanism is known to have singular loci within its workspace affecting its use. In this paper, singularity avoidance of the 3-RRR mechanism using kinematic redundancy is presented. First, singularity analysis of the proposed 3-RPRR mechanism is described and a simple and effective redundancy resolution algorithm based on local optimization suitable for real-time control is developed. Here, the cost function in the optimization is designed to avoid the most problematic singularity configurations, where the end-effector can be locally moved even though all actuated joints are locked. Results from simulation show that the resultant 3-RPRR mechanism can be used to avoid singularities associated with the 3-RRR mechanism, and enlarges the usable workspace.

I. Introduction

IT is well known that the 3-RRR mechanism is a practical planar parallel manipulator since its structure is simple and the actuators are fixed at the base, which reduces the inertia of the moving body. Also, as a parallel mechanism, it has high payload capacity, high accuracy, and high mechanical rigidity. However, the 3-RRR mechanism has a serious disadvantage to overcome: singular loci of the mechanism exist within its workspace. Obviously, singular configurations of a mechanism may result in serious problems, and those configurations must be avoided.

Gosselin and Angeles [1] described a general classification of singularities for closed-loop kinematic chains, and provided the singularity analysis of the 3-RRR mechanism as an example. According to Bonev and Gosselin [2], for constant payload orientation, the singularity loci of the 3-RRR mechanism within its workspace can be represented by curves of degree 42. The most feasible methods for dealing with singularity avoidance of the 3-RRR mechanism are to utilize actuator redundancy [3-13] or kinematic redundancy [14-17]. Actuator redundancy means that the mobility of a manipulator is less than the number of actuated joints.

Manuscript received September 15, 2006. The authors gratefully acknowledge the Division of Research and Innovation of the California Department of Transportation which has supported this work through the Advanced Highway Maintenance and Construction Technology (AHMCT) Research Center at the University of California, Davis.

The authors are with the AHMCT Research Center, Department of Mechanical & Aeronautical Engineering, University of California-Davis, Davis, CA 95616 USA. Author emails: scha@ucdavis.edu, talasky@ucdavis.edu, and savelinsky@ucdavis.edu. Corresponding author, S.A. Velinsky.

In order to reduce singular configurations, Firmani and Podhorodeski [10] used actuator redundancy by replacing some passive revolute joints of the 3-RRR mechanism with actuated ones. However, actuator redundancy results in challenging internal force problems, which means that a mechanism cannot be controlled with only position control scheme.

A manipulator has kinematic redundancy when its mobility is larger than the number of degrees of freedom (DOF) needed to set an arbitrary position and orientation of its end-effector. In an attempt to avoid singularities inside the 3-RRR mechanism's workspace, this paper proposes implementation of kinematic redundancy. Obviously, using the introduced extra DOF, the redundant mechanism can execute the primary task while concurrently avoiding singularities. However, detailed algorithms for kinematic redundancy resolution related to the 3-RRR mechanism have not been published. In this paper, a new redundant planar mechanism is proposed and a kinematic redundancy resolution algorithm for the proposed mechanism is developed based on local optimization techniques suitable for real-time control.

II. Introduction of Additional Mobility to the 3-RRR Mechanism

Fig. 1 shows the schematic diagram of the proposed planar 3-RPRR mechanism, which is the same architecture as the 3-RRR mechanism except with added redundant active prismatic joints. The mechanism consists of an equilateral triangular moving platform $B_1B_2B_3$, and three legs $O_iA_iB_i$ for $i = 1, 2, 3$. Each leg is fixed at the base (point O_i) by an actuated revolute joint and connected to the moving platform at point B_i by a passive revolute joint. Point O_i is located on the vertices of an equilateral triangle $O_1O_2O_3$. Link O_iA_i consists of two sub-links which are connected by an actuated prismatic joint. Links O_iA_i and A_iB_i are connected with a passive revolute joint. A Cartesian coordinate system xy is attached to the base at point O_1. It is assumed that the position of point P (the centroid of the moving platform) with respect to the reference frame represents the position of the moving platform $B_1B_2B_3$ and the orientation of the moving platform is described by the angle α between $\overline{O_1O_2}$ (x-axis) and $\overline{B_1B_2}$.

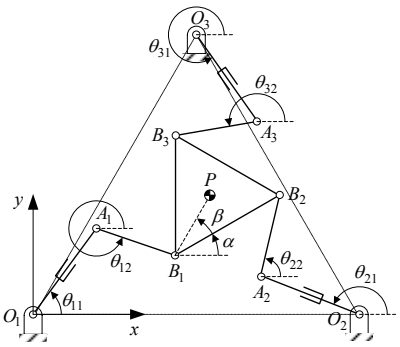

Fig. 1. Schematic diagram of the 3-RPRR mechanism.

III. Singularity Analysis of the 3-RPRR Mechanism

For singularity analysis of a parallel mechanism, assuming that **p** is the $(n\times 1)$ task space vector and **q** is the $(m\times 1)$ active joint space vector, the kinematic relationship between **p** and **q** can be described as

$$\mathbf{f}(\mathbf{p},\mathbf{q})=\mathbf{0}, \tag{1}$$

where **f** is an *n*-dimensional function of **p** and **q**. Differentiating (1) with respect to time gives

$$\mathbf{A}\dot{\mathbf{p}}+\mathbf{B}\dot{\mathbf{q}}=\mathbf{0}, \tag{2}$$

where $\mathbf{A}=\partial\mathbf{f}/\partial\mathbf{p}$ and $\mathbf{B}=\partial\mathbf{f}/\partial\mathbf{q}$ are $(n\times n)$ and $(n\times m)$ matrices, respectively. According to singularity analysis for a non-redundant parallel mechanism $(n=m)$ by Gosselin and Angeles [1], there are three types of singularities. The first type arises when $\det(\mathbf{B})=0$. These singularities correspond to the mechanism configurations in which the end-effector is located on a boundary of the workspace. The second type of singularity occurs when $\det(\mathbf{A})=0$. In the case of the 3-RRR mechanism, when the lines aligned with link A_iB_i for $i=1,2,3$ intersect at a single point or are all parallel, the second type of singularity occurs. The third type of singularity occurs when both **A** and **B** are singular. It is noted that the most problematic singularity is the second type of singularity, since at this type of singularity configuration located inside of the workspace, the end-effector can move even though all the actuated joints are locked. Thus, this paper focuses on avoidance of only the second type of singularity.

Now, consider the kinematic constraints of the 3-RRR mechanism. In Fig. 1, θ_{i1} and θ_{i2} $(i=1,2,3)$ represent the angular positions of links O_iA_i and A_iB_i with respect to the x-axis of the reference frame, respectively. Then, the kinematic constraints for the legs can be obtained as follows:

For leg 1,

$$x=l_{11}\cos\theta_{11}+l_{12}\cos\theta_{12}+l_{13}\cos(\alpha+\beta), \tag{3}$$

$$y=l_{11}\sin\theta_{11}+l_{12}\sin\theta_{12}+l_{13}\sin(\alpha+\beta). \tag{4}$$

For leg 2,

$$x=L+l_{21}\cos\theta_{21}+l_{22}\cos\theta_{22}-l_{23}\cos(\beta-\alpha), \tag{5}$$

$$y=l_{21}\sin\theta_{21}+l_{22}\sin\theta_{22}+l_{23}\sin(\beta-\alpha). \tag{6}$$

For leg 3,

$$x=L/2+l_{31}\cos\theta_{31}+l_{32}\cos\theta_{32}-l_{33}\cos(\alpha+3\beta), \tag{7}$$

$$y=\sqrt{3}L/2+l_{31}\sin\theta_{31}+l_{32}\sin\theta_{32}-l_{33}\sin(\alpha+3\beta). \tag{8}$$

Here, l_{i1} and l_{i2} denote the lengths of link O_iA_i and A_iB_i, respectively, while l_{i3} and L represent the lengths of $\overline{B_iP}$ and $\overline{O_1O_2}$, respectively (both constant).

For leg 1, to eliminate the terms which include the passive joint variable θ_{12}, (3) and (4) can be rewritten as

$$x-l_{11}\cos\theta_{11}-l_{13}\cos(\alpha+\beta)=l_{12}\cos\theta_{12}, \tag{9}$$

$$y-l_{11}\sin\theta_{11}-l_{13}\sin(\alpha+\beta)=l_{12}\sin\theta_{12}. \tag{10}$$

Summing the squares of (9) and (10) gives

$$\left[x-l_{11}\cos\theta_{11}-l_{13}\cos(\alpha+\beta)\right]^2+\left[y-l_{11}\sin\theta_{11}-l_{13}\sin(\alpha+\beta)\right]^2=l_{12}^2. \tag{11}$$

A similar derivation for (5) - (8) yields

$$\left[x-L-l_{21}\cos\theta_{21}+l_{23}\cos(\beta-\alpha)\right]^2+\left[y-l_{21}\sin\theta_{21}-l_{23}\sin(\beta-\alpha)\right]^2=l_{22}^2, \tag{12}$$

$$\left[x-L/2-l_{31}\cos\theta_{31}+l_{33}\cos(\alpha+3\beta)\right]^2+\left[y-\sqrt{3}L/2-l_{31}\sin\theta_{31}+l_{33}\sin(\alpha+3\beta)\right]^2=l_{32}^2. \tag{13}$$

Differentiating (11)-(13) with respect to time, the kinematic relationship of (2) between **p** and **q** is obtained with

$$\mathbf{p}=\begin{bmatrix}x & y & \alpha\end{bmatrix}^T, \tag{14}$$

$$\mathbf{q}=\begin{bmatrix}l_{11} & \theta_{11} & l_{21} & \theta_{21} & l_{31} & \theta_{31}\end{bmatrix}^T, \tag{15}$$

$$\mathbf{A}=\begin{bmatrix}a_{11} & a_{12} & a_{13}\\ a_{21} & a_{22} & a_{23}\\ a_{31} & a_{32} & a_{33}\end{bmatrix}, \tag{16}$$

$$\mathbf{B}=\begin{bmatrix} b_{11} & b_{12} & 0 & 0 & 0 & 0 \\ 0 & 0 & b_{23} & b_{24} & 0 & 0 \\ 0 & 0 & 0 & 0 & b_{35} & b_{36} \end{bmatrix}, \quad (17)$$

where

$$a_{11}=x-l_{11}\cos\theta_{11}-l_{13}\cos(\alpha+\beta)=l_{12}\cos\theta_{12}, \quad (18)$$

$$a_{12}=y-l_{11}\sin\theta_{11}-l_{13}\sin(\alpha+\beta)=l_{12}\sin\theta_{12}, \quad (19)$$

$$a_{13}=l_{13}\left[a_{11}\sin(\alpha+\beta)-a_{12}\cos(\alpha+\beta)\right], \quad (20)$$

$$a_{21}=x-L-l_{21}\cos\theta_{21}+l_{23}\cos(\beta-\alpha)=l_{22}\cos\theta_{22}, \quad (21)$$

$$a_{22}=y-l_{21}\sin\theta_{21}-l_{23}\sin(\beta-\alpha)=l_{22}\sin\theta_{22}, \quad (22)$$

$$a_{23}=l_{23}\left[a_{21}\sin(\beta-\alpha)+a_{22}\cos(\beta-\alpha)\right], \quad (23)$$

$$a_{31}=x-L/2-l_{31}\cos\theta_{31}+l_{33}\cos(\alpha+3\beta)= l_{32}\cos\theta_{32}, \quad (24)$$

$$a_{32}=y-\sqrt{3}L/2-l_{31}\sin\theta_{31}+l_{33}\sin(\alpha+3\beta)= l_{32}\sin\theta_{32}, \quad (25)$$

$$a_{33}=-l_{33}\left[a_{31}\sin(\alpha+3\beta)-a_{32}\cos(\alpha+3\beta)\right], \quad (26)$$

and for $i=1,2,3$ and $j=2(i-1)+1$,

$$b_{ij}=-\left(a_{i1}\cos\theta_{i1}+a_{i2}\sin\theta_{i1}\right), \quad (27)$$

$$b_{i(j+1)}=l_{i1}\left(a_{i1}\sin\theta_{i1}-a_{i2}\cos\theta_{i1}\right). \quad (28)$$

Similarly to the case for non-redundant parallel manipulators, when the determinant of $\mathbf{A}$ in (16) is equal to zero, the second type of singularity of the 3-RPRR mechanism occurs.

IV. Formulation of the Kinematic Redundancy Resolution Algorithm

For a given position and orientation of the moving platform, infinite feasible configurations can be found due to the kinematic redundancy of the 3-RPRR mechanism. Here, to resolve the redundancy, i.e. to choose one among the set of possible mechanism configurations, local optimization suitable for real-time control is applied. As described in the previous section, the most problematic singularity is the second type of singularity, since in these configurations the end-effector can be locally moved even though all actuated joints are locked. Therefore, the local optimization criterion in the proposed algorithm is to avoid $\det(\mathbf{A})=0$.

Assuming that a desired task space variable vector $\mathbf{p}_k$ is given at time index k (for a sampled data system with sample period T), the proposed kinematic redundancy resolution algorithm can be summarized as follows. When the value of $\det(\mathbf{A})$ at the initial configuration is negative (positive), minimizing (maximizing) the cost function

$$H=\det(\mathbf{A}_k), \quad (29)$$

subject to the increment limitation

$$l_{i1,k-1}-\Delta l_{i1}\le l_{i1,k}\le l_{i1,k-1}+\Delta l_{i1},\ i=1,2,3, \quad (30)$$

where Δl_{i1} is determined based on the feasible maximum velocity $\bar{v}_i$ of the prismatic joints, i.e. $\Delta l_{i1}=\bar{v}_i T$.

As shown in (18)-(26), $\det(\mathbf{A})$ is a function of six active joint variables l_{i1} and θ_{i1} for $i=1,2,3$. However, supposing l_{i1} is known, θ_{i1} can be written as a function of l_{i1} as follows. For leg i, from (18) and (19), (21) and (22), or (24) and (25),

$$l_{i1}\cos\theta_{i1}+l_{i2}\cos\theta_{i2}=C_i, \quad (31)$$

$$l_{i1}\sin\theta_{i1}+l_{i2}\sin\theta_{i2}=D_i, \quad (32)$$

where

$$C_1=x-l_{13}\cos(\alpha+\beta), \quad (33)$$

$$D_1=y-l_{13}\sin(\alpha+\beta), \quad (34)$$

$$C_2=x-L+l_{23}\cos(\beta-\alpha), \quad (35)$$

$$D_2=y-l_{23}\sin(\beta-\alpha), \quad (36)$$

$$C_3=x-L/2+l_{33}\cos(\alpha+3\beta), \quad (37)$$

$$D_3=y-\sqrt{3}L/2+l_{33}\sin(\alpha+3\beta), \quad (38)$$

and, obviously, C_i and D_i are constants for a given configuration of the mechanism.

From (31) and (32), θ_{i1} can be computed as

$$\theta_{i1}=\tan^{-1}\left(D_i/C_i\right)+\cos^{-1}\left(E_i\right), \quad (39)$$

where

$$E_i=\frac{l_{i1}^2-l_{i2}^2+C_i^2+D_i^2}{2l_{i1}\sqrt{C_i^2+D_i^2}}. \quad (40)$$

Here, it is assumed that the 3-RPRR mechanism will operate in one working mode or branch, as shown in Fig. 1.

Thus, the cost function H for optimization is given by a function of l_{i1} $(i = 1, 2, 3)$. Fig. 2 provides a flowchart for the kinematic redundancy resolution algorithm based on local optimization for singularity avoidance. In Fig. 2, δ represents an input variable which determines the time to start to control the prismatic joints of the 3-RPRR mechanism. This value is related to measures of proximity of a configuration to a singularity [18]. Since these measures are not the subject of this paper, δ is herein assumed constant.

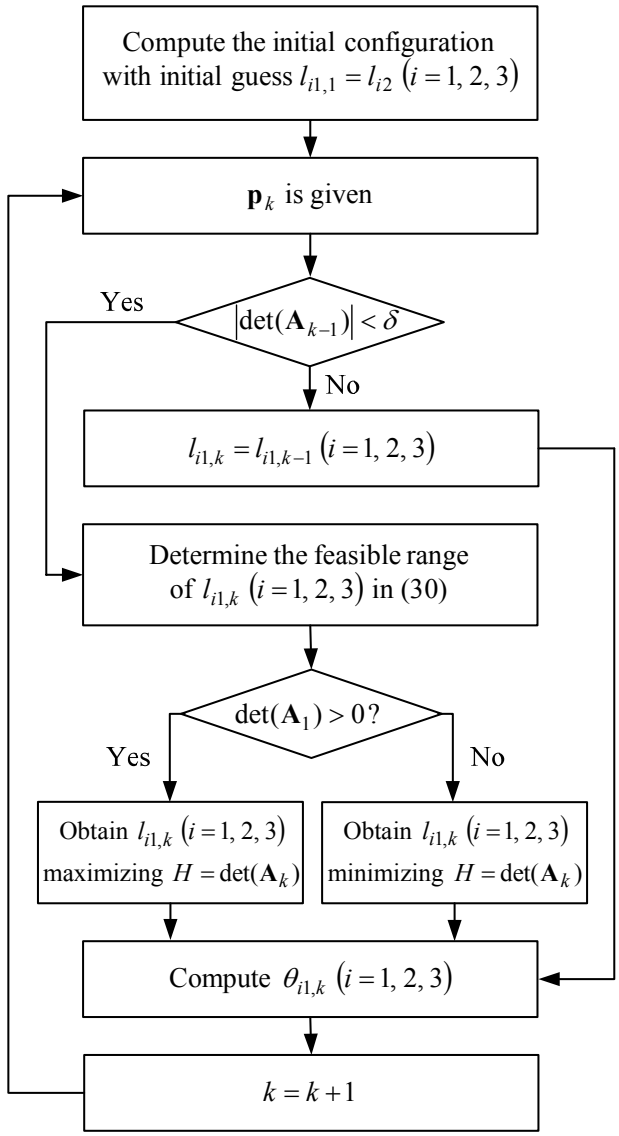

Fig. 2. Flowchart of the proposed kinematic redundancy resolution algorithm.

V. SIMULATION

In this section, a simulation example is shown to verify the proposed algorithm. The same desired trajectory is used for comparison of the 3-RPRR mechanism with the 3-RRR mechanism. To match one of the 3-RRR mechanisms presented in Bonev and Gosselin [2], the geometric parameters of the 3-RRR mechanism are assumed as (for $i = 1, 2, 3$)

$$l_{i1} = l_{i2} = 1, \; l_{i3} = 0.513 \text{ m}, \tag{41}$$

and

$$L = 1.714 \text{ m}. \tag{42}$$

The geometric parameters of the 3-RPRR mechanism are: (for $i = 1, 2, 3$)

$$0.75 \le l_{i1} \le 1.5, \; l_{i2} = 1, \; l_{i3} = 0.513 \text{ m}, \tag{43}$$

and

$$L = 1.714 \text{ m}. \tag{44}$$

For the example, the desired trajectory is an arc given by

$$\theta_k = (V/R)kT \text{ rad}, \; (k = 1, 2, \cdots 3900 \text{ and } T = 1 \text{ ms}), \tag{45}$$

$$x_k = L/2 - R + R\cos\theta_k \text{ m}, \tag{46}$$

$$y_k = \sqrt{3}L/6 + R\sin\theta_k \text{ m}, \tag{47}$$

where V denotes the desired speed of the end-effector and R represents the radius of the arc. In this example, V and R are assumed to be 0.3 m/s and 0.75 m, respectively. Also, α_k is fixed at $\pi/12$ rad. Fig. 3 shows the desired trajectory and the initial configuration for both mechanisms' simulation.

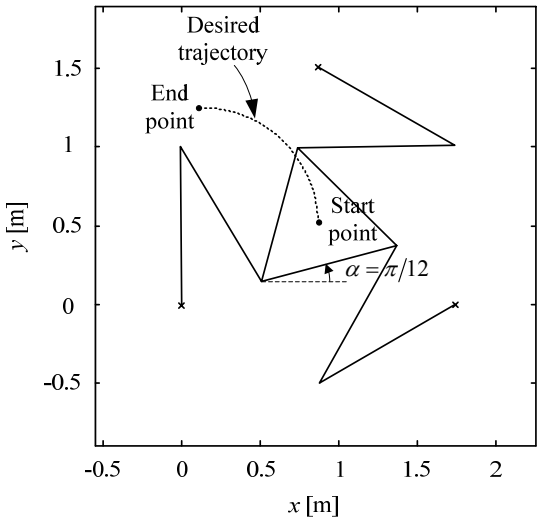

Fig. 3. Desired trajectory and initial configuration

Figs. 4 and 5 show the simulation results of the 3-RRR mechanism. In Fig. 4, when t = 1.56 sec, $\det(\mathbf{A}) = 0$, i.e. the

configuration of the mechanism is singular. The singular configuration at $t = 1.56$ sec is illustrated in Fig. 5. Because the lines along links A_iB_i $(i = 1, 2, 3)$ intersect at a point, the second type of singularity occurs.

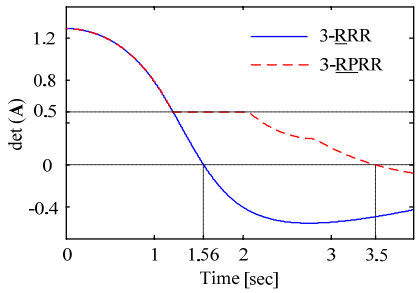

Fig. 4. Variation of det(**A**) for the two mechanisms.

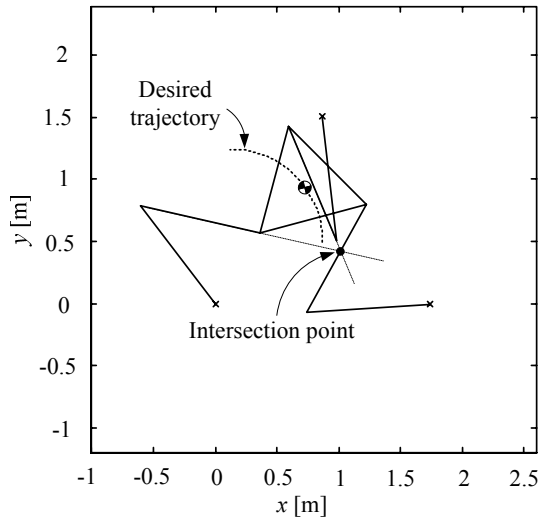

Fig. 5. Singular configuration of the 3-RRR mechanism at t = 1.56 sec.

Assume the prismatic joints of the 3-RPRR mechanism consist of a motor and a ball-screw mechanism. Based on a practical system configuration, it is assumed that the maximum motor speed is 2500 rpm and the screw lead is 0.008 m. Then, Δl_{i1} for $i = 1, 2, 3$ is computed as 3.3×10^{-4} m. Based on the flowchart in Fig. 2, $l_{i1,1}$ is given as 1 m. Also, δ is assumed to be 0.5.

The simulation results of the 3-RPRR mechanism are shown in Figs. 4, 6, and 7. In Fig. 4, $\det(\mathbf{A}) = 0$ at $t = 3.5$ sec. In Fig. 6, since the lines aligned with link A_iB_i $(i = 1, 2, 3)$ intersect at a point, the second type of singularity occurs. Because of the moving ranges of the prismatic joints, the singularity configuration in Fig. 6 cannot be avoided. However, comparing the results in Fig. 4, it is evident that the end-effector of the 3-RPRR mechanism moved farther without meeting a singularity than for the 3-RRR mechanism. Fig. 7 shows the variation of l_{i1} $(i = 1, 2, 3)$. Here, for optimization, the *fmincon* routine from the MATLAB optimization toolbox is used on a PC with 1.7 GHz CPU. The maximum and mean computation times are about 41 ms and 15 ms, respectively.

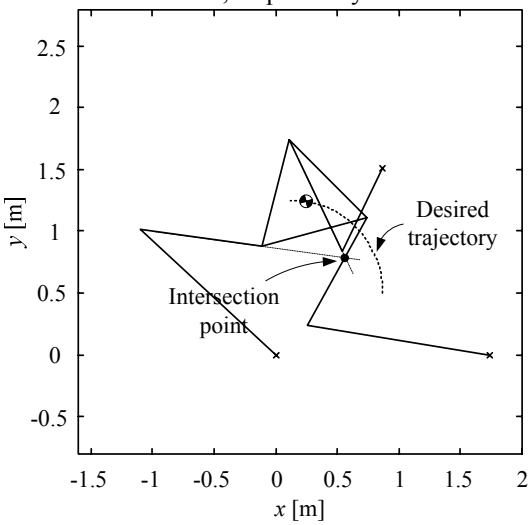

Fig. 6. Singular configuration of the 3-RPRR mechanism at $t = 3.5$ sec.

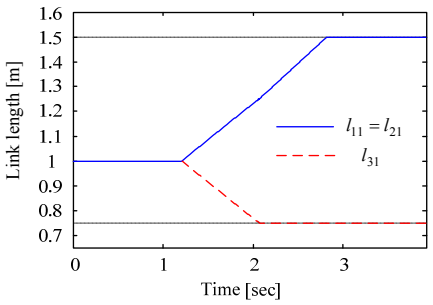

Fig. 7. Link-length variation for the 3-RPRR mechanism.

Due to kinematic redundancy, the singularity-free workspace of the 3-RPRR mechanism can be identified only when desired trajectories of the end-effector are given. For example, consider the identical 3-RPRR mechanism used in the previous example. When desired trajectories are given as lines with $\alpha_k = \pi/4$ rad, the singularity-free workspace of the 3-RPRR mechanism can be approximately obtained as shown in Fig. 8. Here, between line samples, linear interpolation is applied. Fig. 9 shows a comparison of the two mechanisms' singularity-free workspaces. With denser sampling, the workspace borders will be almost continuous. Although compactness of the singularity-free workspaces has not been proven, it is apparent that kinematic redundancy introduced to the 3-RRR mechanism can be used to increase its singularity-free workspace.

VI. CONCLUSIONS

In this paper, singularity avoidance of the 3-RRR mechanism using kinematic redundancy was presented. A simple and effective redundancy resolution algorithm was developed based on local optimization. Here, the cost function in the optimization was designed to avoid the most problematic singularity configurations, where the end-

effector can be moved locally even though all actuated joints are locked. The comparison results with the 3-RRR mechanism show the kinematic redundancy of the 3-RPRR mechanism can be used to avoid singularities. In other words, this approach can effectively increase the singularity-free workspace. In addition, due to its relatively light computational cost, this approach provides an alternative to methods that use actuator redundancy for singularity avoidance, and is well-suited for real-time applications. In future work, the authors are evaluating performance for singularity avoidance of kinematically redundant planar parallel mechanisms (for example, the 3-RRPR or 3-RPRPR mechanisms), theoretical compactness of workspaces, and issues of global vs. local optimization.

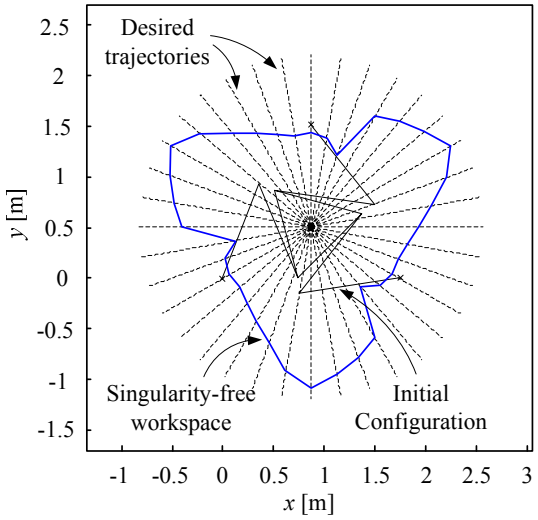

Fig. 8. Approximate singularity-free workspace of the 3-RPRR mechanism.

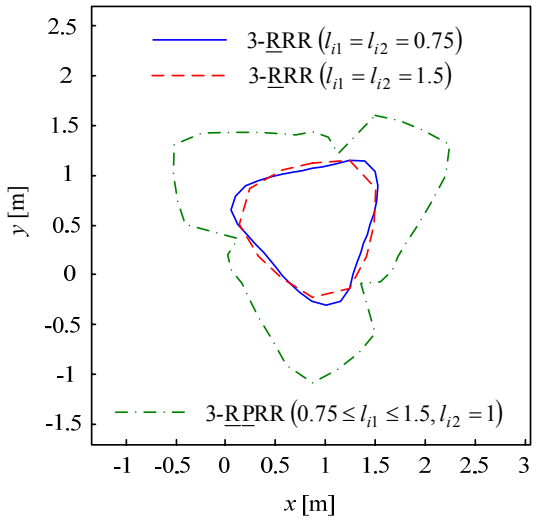

Fig. 9. Comparison of the two mechanisms' singularity-free workspaces.

REFERENCES

[1] C. Gosselin and J. Angeles, "Singularity Analysis of Closed-Loop Kinematic Chains," *IEEE Transactions on Robotics and Automation*, vol. 6, no. 3, pp. 281-290, 1990.

[2] I.A. Bonev and C. Gosselin, "Singularity Loci of Planar Parallel Manipulators With Revolute Joints," in *2nd Workshop on Computational Kinematics*, Seoul, Korea, 2001, pp. 291-299.

[3] M.A. Nahon and J. Angeles, "Reducing the Effect of Shocks Using Redundant Actuation," in *IEEE Conference on Robotics and Automation*, Sacramento, CA, 1991, pp. 238-243.

[4] R. Kurtz and V. Hayward, "Multiple-Goal Kinematic Optimization of Parallel Spherical Mechanism with Actuator Redundancy," *IEEE Transactions on Robotics and Automation*, vol. 8, no. 5, pp. 644-651, 1992.

[5] B. Dasgupta and T.S. Mruthyunjaya, "Force Redundancy in Parallel Manipulators: Theoretical and Practical Issues," *Mechanism and Machine Theory*, vol. 33, no. 6, pp. 727-742, 1998.

[6] J.F. O'Brien and J.T. Wen, "Redundant Actuation for Improving Kinematic Manipulability," in *IEEE Conference on Robotics and Automation*, Detroit, MI, 1999, pp. 1520-1525.

[7] S. Kock and W. Schumacher, "Control of a Fast Parallel Robot with a Redundant Chain and Gear Boxes: Experimental Results," in *IEEE Conference on Robotics and Automation*, San Francisco, CA, 2000, pp. 1924-1929.

[8] S.H. Lee, B.-J. Yi, S.H. Kim, and Y.K. Kwak, "Control of Impact Disturbance by a Redundantly Actuated Mechanism," in *IEEE Conference on Robotics and Automation*, Seoul, Korea, 2001, pp. 3734 - 3741.

[9] H. Cheng, Y.-K. Yiu, and Z. Li, "Dynamics and Control of Redundantly Actuated Parallel Manipulators," *IEEE/ASME Transactions on Mechatronics*, vol. 8, no. 4, pp. 483-491, 2003.

[10] F. Firmani and R.P. Podhorodeski, "Force-Unconstrained Poses for a Redundantly-Actuated Planar Parallel Manipulator," *Mechanism and Machine Theory*, vol. 39, no. 5, pp. 459-476, 2004.

[11] S. Krut, O. Company, and F. Pierrot, "Velocity Performance Indices for Parallel Mechanisms with Actuation Redundancy," *Robotica*, vol. 22, no. 2, pp. 129-139, 2004.

[12] A. Muller, "Internal Preload Control of Redundantly Actuated Parallel Manipulators-Its Application to Backlash Avoiding Control," *IEEE Transactions on Robotics*, vol. 21, no. 4, pp. 668-677, 2005.

[13] S.B. Nokleby, R. Fisher, R.P. Podhorodeski, and F. Firmani, "Force Capabilities of Redundantly-Actuated Parallel Manipulators," *Mechanism and Machine Theory*, vol. 40, no. 5, pp. 578-599, 2005.

[14] K.E. Zanganeh and J. Angeles, "Mobility and Position Analyses of a Novel Redundant Parallel Manipulator," in *IEEE Conference on Robotics and Automation*, San Diego, CA, 1994, pp. 3049-3054.

[15] J. Wang and C. Gosselin, "Kinematic Analysis and Design of Kinematically Redundant Parallel Mechanisms," *Journal of Mechanical Design*, vol. 126, no. 1, pp. 109-118, 2004.

[16] M.G. Mohamed and C. Gosselin, "Design and Analysis of Kinematically Redundant Parallel Manipulators with Configurable Platforms," *IEEE Transactions on Mechatronics*, vol. 21, no. 3, pp. 277-287, 2005.

[17] S.-H. Cha, T.A. Lasky, and S.A. Velinsky, "Kinematic Redundancy Resolution for Serial-Parallel Manipulators via Local Optimization Including Joint Constraints," *Mechanics Based Design of Structures and Machines*, vol. 34, no. 2, pp. 213-239, 2006.

[18] P.A. Voglewede and I. Eber-Uphoff, "Overarching Framework for Measuring Closeness to Singularities of Parallel Manipulators," *IEEE Transactions on Mechatronics*, vol. 21, no. 6, pp. 1037-1045, 2005.